

SUPPORTING INFORMATION

Analysis of Powders Containing Illicit Drugs Using Magnetic Levitation

Christoffer K. Abrahamsson, Amit Nagarkar, Michael J. Fink, Daniel J. Preston, Shencheng Ge,

Joseph S. Bozenko Jr.,* and George M. Whitesides*

ABSTRACT: Magneto-Archimedes levitation (MagLev) enables the separation of powdered mixtures of illicit drugs (cocaine, methamphetamine, heroin, fentanyl and its analogs), adulterants, and diluents based on density, and allows the presumptive identification of individual components. Small samples (mass <50 mg), with low concentrations of psychoactive drugs, present a particular challenge to analysis for forensic chemists. The MagLev device—a cuvette containing a solution of paramagnetic gadolinium(III) chelate in a non-polar solvent, placed between two like-poles-facing NdFeB magnets—allowed separation of seven relevant compounds simultaneously. For example, initial separation with MagLev, followed by characterization by FTIR-ATR, enabled identification of fentanyl in a sample of fentanyl-laced heroin (1.3 wt% fentanyl, 2.6 wt% heroin, and 96.1 wt% lactose). MagLev allows identification of unknown powders in mixtures and enables confirmatory identification based on structure-specific techniques.

[*] Dr. C.K. Abrahamsson, Dr. A. Nagarkar, Dr. M. J. Fink, Dr. D. J. Preston, Dr. S. Ge, Prof. G. M. Whitesides
Department of Chemistry and Chemical Biology
Harvard University
E-mail: gwhitesides@gmwgroup.harvard.edu
Website: <https://gmwgroup.harvard.edu/>

[*] J. S. Bozenko Jr.
Special Testing and Research Laboratory
Drug Enforcement Administration (DEA)
Dulles, VA
E-mail: jsbozenko@dea.usdoj.gov

Prof. G. M. Whitesides
Wyss Institute for Biologically Inspired Engineering
Harvard University
60 Oxford St., Cambridge, MA 02138

Prof. G. M. Whitesides
Kavli Institute for Bionano Inspired Science and Technology
Harvard University, 29 Oxford Street, MA 02138

Supporting information for this article is given via a link at the end of the document.

TABLE OF CONTENTS

1. TABLE OF CONTENTS.....	2
2. THEORY.....	4
Figure S1. The Maglev device and the custom-made cuvette.....	5
Figure S2. Schematic diagram illustrating the relevant forces during MagLev.....	6
3. EXPERIMENTAL PROCEDURES	
3.1 Construction of the MagLev Device.....	7
3.2 Synthesis of the Gd(DPM)₃TOPO-Chelate Complex.....	7
3.3 Synthesis of the Gd(acac)₃TOPO-Chelate Complex.....	8
3.4 Performance of the Gd(DPM)₃TOPO as a Paramagnetic Solution for MagLev Separation.....	9
3.5 Safety and Handling of the Paramagnetic Solution.....	10
3.6 Powdered Illicit Drugs, Adulterants, and Diluents.....	12
3.7 Measurement of Density of Powders with MagLev.....	12
3.8 Density-based Separation of Powders using MagLev.....	13
Figure S3. Schematic diagram of the custom cuvette.....	14
3.9 A Model System Based on Lidocaine·HCl and Caffeine.....	14
3.10 ¹H-NMR Analysis of Fractions of Powders Separated by MagLev.....	15
3.11 FTIR-ATR Analysis of Fractions of Powders Separated by MagLev.....	16
3.12 FTIR-ATR Analysis of the Paramagnetic Complexes.....	16
3.13 Scanning Electron Microscopy Imaging of Powders.....	17
3.14 Image Processing.....	18

4. LITERATURE, RESULTS AND DISCUSSION

Table S1. Names and molecular structures of compounds found in mixtures of drugs...19

Table S2. Common ranges of purity of illicit drugs at the retail level.....22

Table S3. Recommendations and categorization of techniques used in identification of illicit drugs.....23

Table S4. The density of the compounds measured in this study compared to literature values.....24

Figure S4. The separation and extraction of the individual components from fentanyl-laced heroin.....25

Scheme S1. The pathways of synthesis for the Gd(DPM)₃TOPO and Gd(acac)₃TOPO complexes.....26

Figure S5. Time lapse photography of individual drugs levitating in the MagLev device.....27

Figure S6. FTIR-ATR spectra from the Gd(DPM)₃TOPO and Gd(acac)₃TOPO complexes.....28

Figure S7. The procedure of density measurements, and standard curves for different paramagnetic solutions in the MagLev.....30

Table S5. Requirements for the handling of scheduled drugs.....31

Figure S8. MagLev separation different organic solvents.....32

Figure S9. Original images presented in Figure 1, 2 and 3 without image processing.....33

5. REFERENCES.....34

6. AUTHOR CONTRIBUTIONS.....36

2. THEORY

A diamagnetic object (e.g., a crystal or a particle from mixture of powdered drugs) achieves a stable levitation height in a paramagnetic solution in an applied magnetic field (we usually use a linear field gradient) when the magnetic force \vec{F}_{mag} the object experiences (as a result of the interaction between the paramagnetic suspending solution and the applied magnetic field) counterbalances its gravitational force \vec{F}_g (corrected for the effect of buoyancy, Figure S2). We describe the theory of MagLev in detail elsewhere.^[1] Eq. S1 gives the levitation height, h (m), of the centroid (volumetric center) of the sample with respect to the surface of the bottom magnet.

$$h = \frac{(\rho - \rho_{medium})g\mu_o d^2}{(\chi - \chi_{medium})4B_o^2} + \frac{d}{2} \quad (Eq\ S1)$$

In Eq. S1, ρ (g cm^{-3}) is the density of the sample, ρ_{medium} (g cm^{-3}) is the density of the paramagnetic solution, χ (unitless) is the magnetic susceptibility of the sample, χ_{medium} (unitless) is the magnetic susceptibility of the paramagnetic solution, g (9.8 m s^{-2}) is the constant of gravitational acceleration, μ_o ($4\pi \times 10^{-7} \text{ N}\cdot\text{A}^{-2}$) is the magnetic permeability of the free space, B_o (T) is the strength of the magnetic field at the center of the top surface of the bottom magnets, and d (m) is the distance of separation between the two like-poles-facing magnets. MagLev is explained in additional detail in previous publications by us and others.^[1-2]

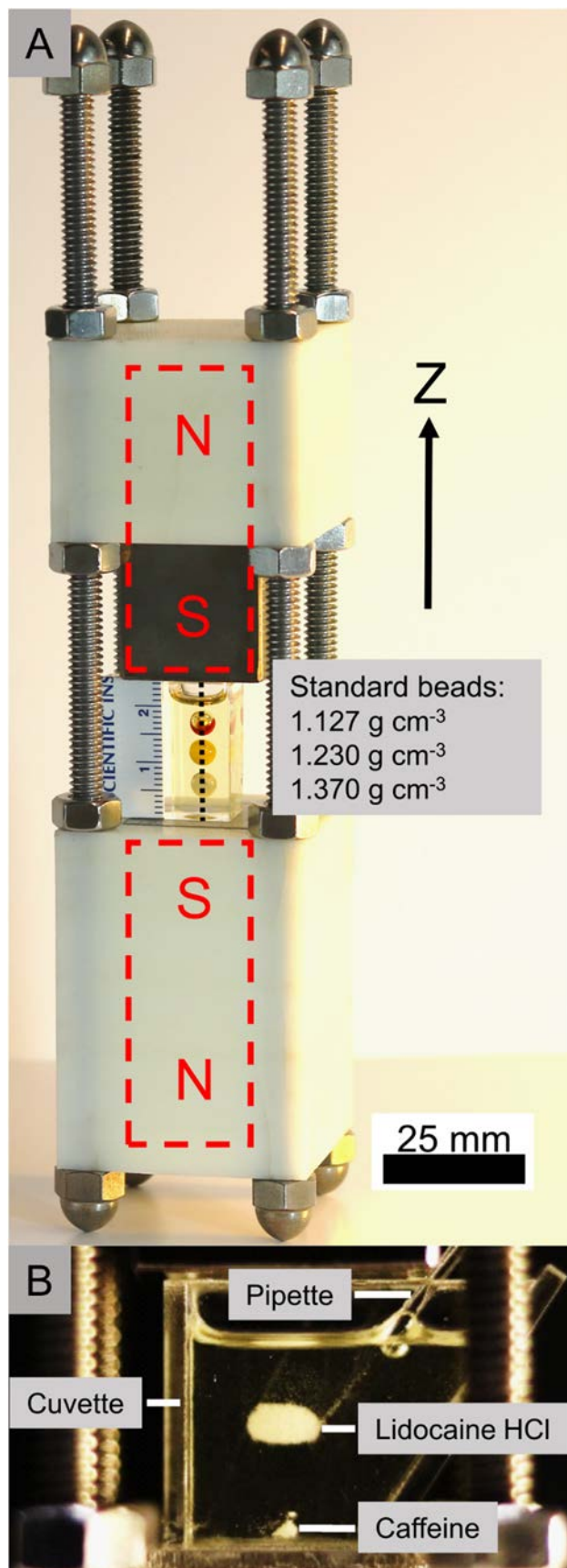


Figure S1. The MagLev device consist of two magnets (red dashed squares) with like-poles facing each other. The magnets are mechanically secured using plastic parts, and steel rods and nuts. The glass beads levitate in a paramagnetic solution. The axis of the magnetic centerline is illustrated by the black dotted line (parallel to the z-direction) between the two magnets. (B) A custom-made plastic cuvette filled with paramagnetic solution sitting in the MagLev device—the shape of this cuvette allows access with a Pasteur pipette from the side of the magnet to extract the separated compounds (A 50-mg mixture consisting of 95 wt% lidocaine·HCl and 5 wt% caffeine after 30 minutes of separation). The paramagnetic solution in both images contain Gd(DPM)₃TOPO (450 mM) dissolved in a mixture of 23 vol% hexane and 77 vol% tetrachloroethylene. The face-to-face separation between the magnets is 25 mm. The images were uniformly post-processed for contrast and clarity.

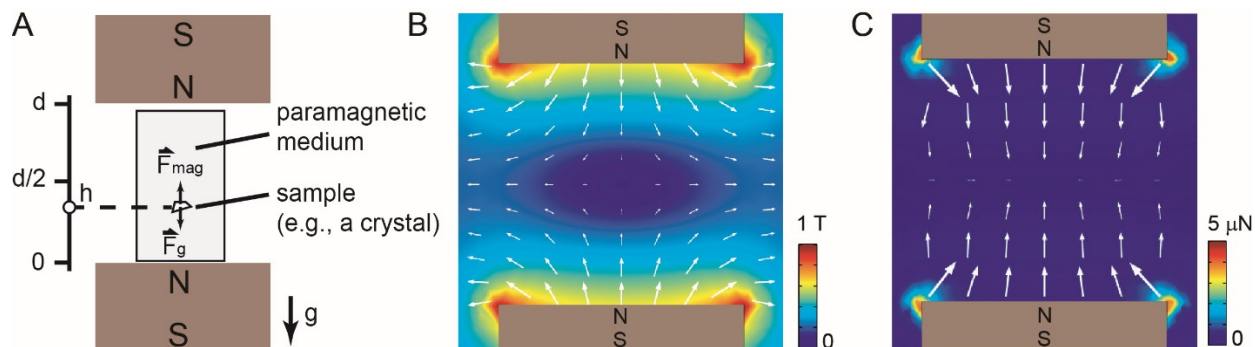


Figure S2. (A) Schematic diagram show the relevant forces during MagLev of powdered mixtures of illicit drugs. (B) Magnetic field B between the magnets (distance of separation 25 mm) of the MagLev device simulated using COMSOL Multiphysics. The color plot shows the strength of the magnetic field, and the white arrows indicate the strength and direction (from N to S) of the magnetic field at the locations of the arrows. (C) Magnetic force (plotted as the logarithm of the magnitude of the force, $\propto \log|F_{mag}| = \log\left|\frac{(\chi_{sample}-\chi_{medium})}{\mu_0}V(\vec{B} \cdot \nabla)\vec{B}\right|$) a sample particle (modeled using a cubic crystal having a side of 100 μm) experiences when suspended in a paramagnetic solution (0.5 M $\text{Gd}(\text{DPM})_3\text{TOPO}$) and placed in the magnetic field shown in (B). The white arrows indicate the strength and direction of the magnetic force acting on the sample at the locations of the arrows. The magnetic force the sample experiences is the result of the attractive interaction of the applied magnetic field and the paramagnetic solution in which the diamagnetic sample is suspended; in comparison, the repulsive interaction between the magnetic field and the diamagnetic sample is orders of magnitude smaller, and thus, can be neglected.

EXPERIMENTAL PROCEDURES

3.1 Construction of the MagLev Device

We have described the design of the MagLev device (device dimensions and weight: $205 \times 45 \times 45$ mm; 700 g).^[3] In brief, it consists of two NdFeB magnets (Neodymium Magnets N42 Block - Dimensions: $25.4 \times 25.4 \times 50.8$ mm, appliedmagnets.com) with like-poles facing each other with a 25.5 mm face-to-face separation resulting in a 0.51 Tesla magnetic field (DC gauss-meter (Model GM1-ST; AlphaLab, Inc., Salt Lake City, UT) at the surface of the magnets (Figure S1). The magnets were mechanically secured in a stand made from (i) acrylonitrile-butadiene-styrene-plastic (ABS-plastic) parts that were designed with computer-aided design (Solidworks™) and printed with a 3D-printer (Stratasys Fortus 250mc, Eden Prairie, MN), (ii) four super-corrosion-resistant 316 stainless steel rods (8" long, 1/4"-20 thread size, McMaster-Carr) and (iii) 16 stainless steel hex nuts (1/4"-20 thread size, McMaster-Carr), and (iv) 8 stainless steel cap nuts (1/4"-20 thread size, McMaster-Carr). The position of the hex nuts along the rods can be adjusted to change the distance between the magnets. The metal parts interact only weakly with the magnets, and cause minimal disturbances to the magnetic field between the two like-poles.

3.2 Synthesis of the Gd(DPM)₃TOPO-Chelate Complex

Tris(dipivaloylmethanato) gadolinium(III) (Gd(DPM)₃; 2.0 g, 2.7 mmol; purchased from Alfa Aesar) was suspended in hexanes or n-heptane (20 mL; 10 mL per gram of starting material) at room temperature. Trioctylphosphine oxide (TOPO; 1.0 g, 2.7 mmol; purchased from Sigma-Aldrich) was added to form a colorless suspension, which became

a clear solution within 10–30 min (depending on batch size). The solution was stirred at room temperature (22°C) for approx. 18 h. The solvent was removed on a rotary evaporator (60°C bath temperature) at reduced pressure (first at 100–25 mbar, then 10^{-3} mbar) to obtain the Gd(DPM)₃TOPO complex as a pale yellow, viscous oil (2.88 g, 2.67 mmol) with a density of approx. 1.1 g/cm³. We have performed this synthesis successfully starting with 1–30 g of Gd(DPM)₃. The yellow color intensifies with larger scales and higher concentrations. The compound was characterized with FTIR-ATR (Figure S6).

The compound is stable for more than one month at 22°C in a capped and air-tight bottle when stored at room temperature in ambient air. Precipitation occurs after extended storage. The precipitate makes the Gd(DPM)₃TOPO oil appear opaque and can be removed by diluting the compound with hexane to 450 mM, and filtering the solution through polyether sulfone syringe filters (0.2 μm, Fisher brand, Thermo Fisher Scientific Inc.). The synthesis and structure of the Gd(DPM)₃TOPO complex is illustrated in Scheme S1A.

3.3 Synthesis of the Gd(acac)₃TOPO-Chelate Complex

Gadolinium(III) acetylacetonate (Gd(acac)₃; 2.3 g, 5.0 mmol), was added to a 50-mL round-bottomed flask attached to a vacuum outlet and trioctylphosphine oxide (TOPO; 2.0 g, 5.2 mmol) was added as a powder. The temperature of this solid mixture was slowly raised to 100°C and kept constant for five minutes. The TOPO melts and solubilizes the Gd(acac)₃. Heating was stopped and a vacuum (150 mbar) was applied for 2 min. Note that heating for longer periods leads to significant darkening of the solution and formation of insoluble precipitates (presumably inorganic polymers). Also, rapid

heating can lead to overheating, and hence the heating step must be conducted slowly (over ~5 minutes). This mixture was cooled to 30–40°C and 1,2-dichloroethylene (4.5 mL) was added. The solution looked turbid. The small amount of insoluble precipitate was removed by filtration using a polysulfone syringe filter (0.4 µm pore size). Filter paper did not work, as pressure is required to filter the relatively viscous solution. This solution was cooled to room temperature to give a faint yellow solution with a density of approx. 1.3 g/cm³. Treatment with active charcoal did not lead to significant improvement in the color of the solution. The compound was characterized with FTIR-ATR (Figure S6).

In an earlier paper^[4], we reported on a gadolinium chelate complex (gadolinium(III) diethylenetriamine triacetic acid didecyldiacetamide, C11-DTTA, m.w. 1107 g mol⁻¹), a hexadentate chelate with at least two free coordination sites on gadolinium(III), which are probably occupied by water. In the absence of stronger ligands this complex dissolved in the organic solvents at concentrations up to approx. 0.4 M, however, above a concentration of 0.2 M the increased viscosity of the solutions (higher viscosity than glycerol) impeded the separation of particles, and caused a large increase in the time required for separation with MagLev.

3.4 Performance of the Gd(DPM)₃TOPO as a Paramagnetic Solution for MagLev Separation

We obtained the Gd(DPM)₃TOPO from the synthesis as a viscous oil, which was fully soluble in hexane, heptane, octane, decane, and tetrachloroethylene within the range of concentrations we tested (34–900 mM). The compound was soluble in other apolar organic solvents as well, such as carbon tetrachloride and cyclohexane. Solution based on

these solvents could all levitate powders (e.g., Figure S8). Solutions with a concentration of up to 450 mM Gd(DPM)₃TOPO had a sufficiently low viscosity to allow for fast equilibration of the powders in the MagLev. Gd(DPM)₃TOPO solutions of higher concentration (>450 mM) became markedly more viscous, increasing the time of the separation.

3.5 Safety and Handling of the Paramagnetic Solution

We chose the combination of hexane and tetrachloroethylene as solvents for the paramagnetic solutions because of their large difference in density (0.65 versus 1.62 g cm⁻³).^[5] The difference allowed for adjustment of the density of the paramagnetic solution by changing the proportion of the solvents. We use chose a halogenated solvent because they are the only non-polar organic solvents that have sufficiently high density (>1.5 g cm⁻³). Both solvents are non-polar and are fully miscible with each other, and with the two types of apolar gadolinium complexes (i.e., Gd(DPM)₃TOPO and Gd(acac)₃TOPO) we used. There are other beneficial properties of these solvents: (i) Their boiling points are significantly higher than room temperature (i.e. n-hexane: 69°C (other suitable n-alkanes was explored, see Figure S8); tetrachloroethylene: 121°C)^[5], but they evaporate in a few minutes after the compounds have been extracted from the MagLev device and placed on a filter paper. (ii) Their low ability to solubilize polar substances (such as the salts of the drugs investigated).^[5] (iii) Their low chemical reactivity.^[5]

The toxicities of the solvents used in the paramagnetic solution are acceptable if handled with the correct safety procedures. The U.S. Hazardous Materials Identification

System rating (HMIS) ranks hexane as a ‘Moderate Hazard’, and tetrachloroethylene as a ‘Serious health Hazard’ for human health (the scale ranges from ‘Minimum Hazard’ to ‘Severe Hazard’).^[5-6]

Hexane is a flammable solvent used in glues, food-oil extraction and chromatography. Inhalation of hexane in air for short time periods can cause mild central nervous system effects, including dizziness, giddiness, slight nausea, and headache. Longer time periods of exposure (e.g., inhalation or contact) to hexane is associated with nerve damage in humans.^[7]

Tetrachloroethylene is a nonflammable solvent that is the most common solvent used in commercial dry-cleaning.^[8] The effect of chronic exposure to tetrachloroethylene can be severe, and the solvent is a suspected carcinogen.^[7a] Precautions should be taken to avoid inhaling the fumes of the tetrachloroethylene and to avoid absorption the solvent through the skin. Tetrachloroethylene and carbon tetrachloride both are rated (HMIS scale) as ‘Severe Hazards’ to human health, however, carbon tetrachloride is a more potent liver toxin.^[9]

Precaution should be taken to reduce the amount of evaporation of solvent from the paramagnetic solution because the faster evaporation of low density hexane solvent relative to the high density tetrachloroethylene solvent and the gadolinium chelate complexes will result in an increase in the density of the paramagnetic solution. The change in density would interfere with the density calibration of the MagLev device. The evaporation of the solvents can be minimized by reducing the time of the separation and by covering the top of the cuvette with aluminum foil. The hexane can also be replaced with solvents with higher boiling point, such as heptane (98°C)^[10], octane (125°C)^[11],

nonane (151°C)^[12], or decane (174°C)^[13] to reduce the rate of evaporation of the solvent.

For examples of separation of powders using MagLev with different n-alkanes, see Figure S8.

3.6 Powdered Illicit drugs, Adulterants, and Diluents

See Table 1. All illicit drugs were produced internally by the Drug Enforcement Administration (DEA) for use as reference materials, except for the heroin·HCl, which came from a seized sample of South American origin. All experiments with illicit drugs were performed at facilities associated with the DEA. All adulterants and diluents were procured from Sigma-Aldrich, St. Louis, MO, except the following: diltiazem hydrochloride (EMD Millipore, Burlington, MA), D-mannitol (Lancaster synthesis, Inc., Windham, NH), papaverine·HCl (ICN Biomedicals, Aurora, OH), and sucrose (EMD Millipore, Burlington, MA). See Table S2 for a list of a chemical names and the molecular structures of all drugs and adulterants.

3.7 Measurement of Density of Powders with MagLev

Disposable UV-grade methacrylate cuvettes (Prod.# Z188018, Sigma Aldrich, outer dimensions 12.7 × 12.7 × 45 mm, inner dimensions: 10 × 10 × 45 mm) were cut with a band saw to a height of 25 mm (~2.5-mL capacity) to fit between the faces of the two magnets. This particular type of plastic cuvette showed good resistance to repeated exposures to the apolar paramagnetic solutions we used. The density gradient was mapped to obtain a standard curve, by recording the height of the levitating glass bead density standards (American Density Materials, Inc. Staunton, VA) of known densities, with a

ruler for reference of distance (Figure S7). The powdered mixtures were prepared by weighing and adding the individual compounds to a 10-mL glass vial and shaking and inverting it by hand for 5 minutes. From these powdered mixtures, samples with weights between 2–50 mg were extracted and added to the cuvette with the paramagnetic solution. The separation of the particles was imaged using a DSLR camera (Canon EOS Rebel T6i with a Canon EF 50 mm f/1.8 STM lens) for single time-point experiments and time-lapse imaging, with a ruler placed next to the cuvette as a reference of position. The levitating powders were illuminated with an external light source. The position of the middle of the centroid of the levitating fractions was used to find the density of the levitating compound from the standard curves.

The time of separation for the powders depends mainly on the following five reasons: (i) The sample size, because large amounts of powder take longer to separate than small samples. (ii) The particle size, because small particles take longer time to separate than large ones. (iii) The concentration of gadolinium(III) in the paramagnetic solution, because a higher concentration of Gd^{3+} results in faster separation. (iv) The viscosity of the paramagnetic solution, because an increase in viscous drag on the particles results in slower separation. (v) The magnetic field strength, because higher magnetic field strength results in faster separation.

3.8 Density-based Separation of Powders using MagLev

We custom-made a larger cuvette (Figure S1B and S3) that allowed access to the levitating powders with a pipette from the side of the MagLev after the powders had equilibrated. The custom cuvette was made by laser cutting (VersaLASER VL-300, Universal Laser Systems, Inc., Scottsdale, AZ) transparent poly(methyl methacrylate)

(PMMA) sheets (2 mm thick, McMaster-Carr Supply Company) and by gluing the sheets together using acrylic adhesive (Weld-On #3 Adhesive, SCIGRIP, Amazon.com). A Pasteur pipette was used to extract the different fractions of powders that had separated in the MagLev (Figure S4). Each fraction was suction filtered on a grade 3 Whatman filter paper, and (at the same time) rinsed with hexane to remove any residues of the $\text{Gd}(\text{DPM})_3\text{TOPO}$.

As expected, powders of compounds of larger particle size (e.g., fentanyl, acetyl-fentanyl, benzyl fentanyl, and heroin) reached their equilibrium positions in the paramagnetic solution faster than compounds of smaller particle size. Compounds present as small particles (cocaine, methamphetamine, and lactose) moved more slowly in the paramagnetic solution (as is consistent with Stoke's law^[14]).

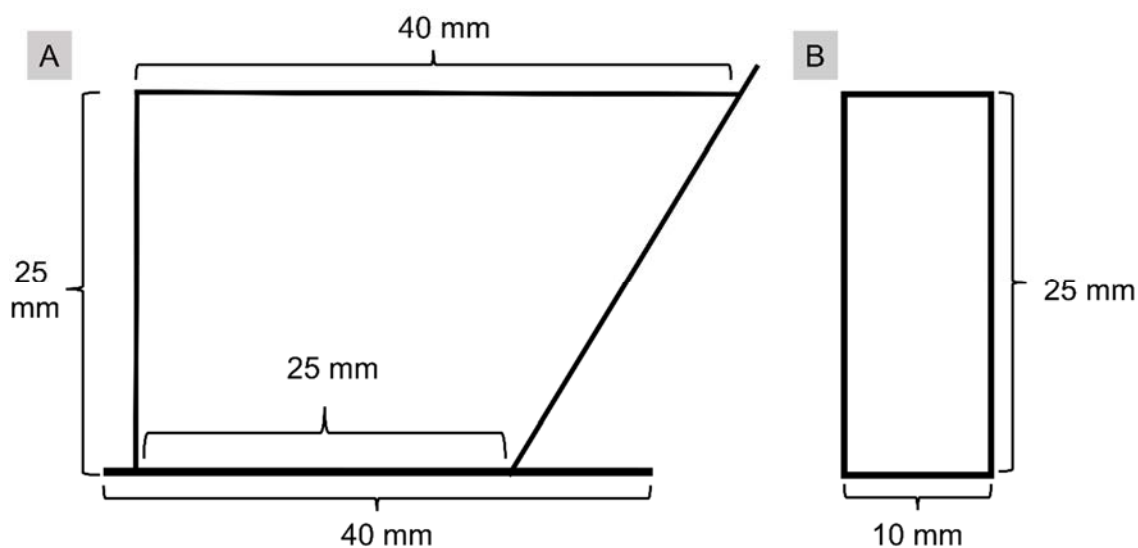


Figure S3. Schematic diagram of the custom cuvette with dimensions viewed from the (A) long side and (B) short side.

3.9 A Model System Based on Lidocaine·HCl and Caffeine

All experiments with active compounds were performed at a DEA facility that had the necessary approvals and infrastructure to allow handling of such compounds. Active compounds are, as expected, associated with significant legal oversight, permits, safety precautions, and limits on the type and amount of compound that can be procured. The bulk of the method development of the MagLev separation took place in the Whitesides laboratory (Department of Chemistry and Chemical Biology, Harvard University), which does not have approval to work with schedule I and II drugs (Table S5).

To facilitate the development of our methodology and the investigation of the dynamics of the separation in the MagLev device we developed a model system that does not contain controlled compounds. The model system consists of a binary mixture of two compounds, lidocaine·HCl and caffeine, both of which are minimally regulated (along with additional benefits) compared to active compounds (chemistry laboratories can buy them without special approval). We chose this model system for the following eight reasons: (i) The two compounds are water-soluble and they thus mimic many active compounds; (ii) Hydrochlorides, such as lidocaine·HCl, are the common salt forms found in seized mixtures of powdered illicit drugs; (iii) Both compounds are commonly found as adulterants in powdered mixtures of illicit drugs; (iv) Laboratories can procure them without special permits and documentation; (v) They have distinctly different densities; (vi) Their particle sizes (in the batches we received) were obviously different when observed by eye; (vii) They are inexpensive (Sigma Aldrich: lidocaine·HCl, Prod.#: PHR1257-500MG, \$127 per gram; caffeine, Prod.#: C0750-5G, \$4 per gram); (viii) Their toxicity is acceptable; i.e., a dust mask is sufficient protection to avoid inhalation of

particles when the dried powders are handled (which is important in the case of lidocaine·HCl).

3.10 $^1\text{H-NMR}$ Analysis of Fractions of Powders Separated by MagLev

A mixture of lidocaine·HCl and caffeine (50:50 wt%) was levitated in the MagLev device until the powders reached their equilibrium levitation heights. The powders were carefully extracted from the cuvette using a Pasteur pipette (guided by pivoting of the hand) and collected by suction filtration on a grade 3 Whatman filter paper. The residue was washed three times with 40 mL portions of solvent (hexane), air-dried, and gently scraped off the filter paper with a spatula and stored in an air-tight glass vial until characterized (up to five days). For $^1\text{H-NMR}$, 3 mg of the residue was dissolved in 0.6 mL of DMSO- d_6 and transferred to a NMR tube for NMR analysis. $^1\text{H-NMR}$ spectra (Figure 3E) were recorded on an Agilent DD2 600 MHz NMR spectrometer, using standard pulse programs.

3.11 FTIR-ATR Analysis of Fractions of Powders Separated by MagLev

The powdered samples that contained powdered lidocaine·HCl and caffeine (same washing procedure as for the $^1\text{H-NMR}$ analysis) were analyzed in their dry, powdered state with FTIR (Figure 3F) with an attenuated total reflection (ATR) diamond window (FTIR-ATR Bruker Platinum, Bruker, Billerica, MA). We measured spectra between 4000–400 cm^{-1} at a resolution of 1 cm^{-1} with 64 sample and background scans. The samples that contained fentanyl·HCl and α -lactose (same washing procedure as for the $^1\text{H-NMR}$ analysis of lidocaine and caffeine) were analyzed with an FTIR-ATR (Nicolet iS19 FTIR with a smart Golden Gate ATR, Thermo-fisher, Madison, WI) between 4000–

455 cm^{-1} at a resolution of 4 cm^{-1} with 64 sample and background scans. The pure compounds (controls) were analyzed without first exposing them to any paramagnetic solutions.

3.12 FTIR-ATR Analysis of the Paramagnetic Complexes

FTIR-ATR (FTIR-ATR Bruker Platinum, Bruker, Billerica, MA) spectrum of the Gd(DPM)₃TOPO (900 mM—as obtained from synthesis) and Gd(acac)₃TOPO (1100 mM in tetrachloroethylene) was recorded by placing a drop of chelate on the ATR diamond window (air set as blank). The spectrum of tetrachloroethylene was measured as a control (air set as blank). All spectra were recorded from 4000–400 cm^{-1} at a resolution of 1 cm^{-1} with 64 sample and background scans (Figure S6). The spectra of the Gd(DPM)₃TOPO and Gd(acac)₃TOPO chelates before and after filtering through activated charcoal showed no significant difference (data not shown), which suggest that the complexes are relatively pure after synthesis.

3.13 Scanning Electron Microscopy Imaging of Powders

To obtain SEM images (Figure 3C), a small amount (<1 mg) of powdered lidocaine·HCl and caffeine were dispensed (on separate SEM stubs) with a spatula directly onto carbon tape (Ted Pella, 16086-12) that had been manually applied to standard SEM stubs (Ted Pella, 16111). The powders were gently pressed with a spatula into the carbon tape to promote adhesion. Field emission electron microscopy was performed on a Zeiss Ultra Plus FESEM (Carl Zeiss, Thornwood, NY) using the in-lens detector at an imaging voltage of 0.8 kV and the SE2 secondary electron detector at an imaging voltage of 6.5 kV.

3.14 Image Processing

Images were edited using Adobe Lightroom. White balance (WB) was manually set, selecting a spot in the darkest and brightest areas of the image for the calibration of the extremes, respectively. Edits were always performed uniformly over the entire area shown in the figures, and with identical settings for every image of the series in Figures 2 and 3. The following parameters were manipulated: color (RGB or monochrome), exposure, contrast, brightness (of highlights, shadows, whites, and blacks), clarity, dehazing, vibrance, and saturation. We show all images in unedited form—WB and exposure as set by the Nikon DSLRs we used—in Figure S9.

4. LITERATURE, RESULTS AND DISCUSSION

Table S1. Trade names, structures, and IUPAC names of the compounds discussed in the paper.

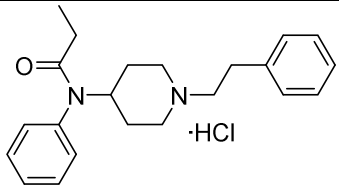
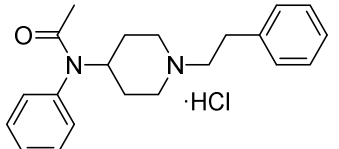
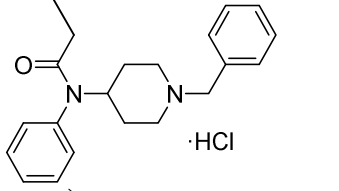
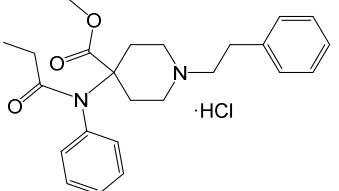
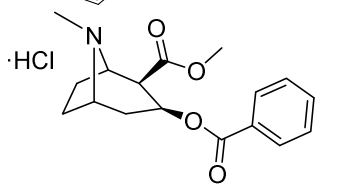
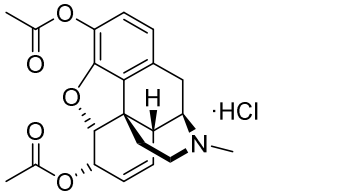
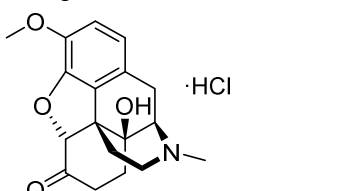
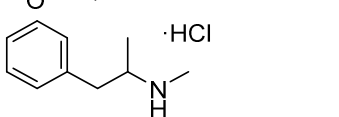
Group	Compound			CAS no.	IUPAC name
	#	Trade name	Structure		
Active compounds	3	Fentanyl-HCl		1443-54-5	N-phenyl-N-[1-(2-phenylethyl)piperidin-4-yl]propanamide; hydrochloride
	4	Acetyl fentanyl-HCl		117332-89-5	N-phenyl-N-[1-(2-phenylethyl)piperidin-4-yl]acetamide; hydrochloride
	5	Benzyl fentanyl-HCl		5156-58-1	N-(1-benzylpiperidin-4-yl)-N-phenyl-propanamide; hydrochloride
	6	Carfentanyl-HCl		59708-52-0 (for base)	Methyl 1-(2-phenylethyl)-4-[phenyl(propanoyl)amino]piperidine-4-carboxylate; hydrochloride
	7	Cocaine-HCl		53-21-4	methyl (1S,3S,4R,5R)-3-benzoyloxy-8-methyl-8-azabicyclo[3.2.1]octane-4-carboxylate; hydrochloride
	8	Heroin-HCl		5893-91-4	[(4R,4aR,7S,7aR,12bS)-9-acetyloxy-3-methyl-2,4,4a,7,7a,13-hexahydro-1H-4,12-methanobenzofuro[3,2-e]isoquinoline-7-yl] acetate; hydrochloride
	9	Oxycodone-HCl		124-90-3	(4R,4aS,7aR,12bS)-4a-hydroxy-9-methoxy-3-methyl-2,3,4,4a,5,6-hexahydro-1H-4,12-methanobenzofuro[3,2-e]isoquinolin-7(7aH)-one; hydrochloride
	10	Methamphetamine HCl		51-57-0	N-methyl-1-phenylpropan-2-amine; hydrochloride

Table S1. Trade names, structures, and IUPAC names of the compounds discussed in the paper.

Group	Compound			CAS no.	IUPAC name
	#	Trade name	Structure		
Adulterants	11	Acetaminophen		103-90-2	N-(4-hydroxyphenyl)acetamide
	12	Caffeine		58-08-2	1,3,7-trimethylpurine-2,6-dione
	13	Diltiazem·HCl		33286-22-5	[(2S,3S)-5-[2-(dimethylamino)ethyl]-2-(4-methoxyphenyl)-4-oxo-2,3-dihydro-1,5-benzothiazepin-3-yl] acetate; hydrochloride
	14	Dipyron / metamizole		5907-38-0	sodium;[(1,5-dimethyl-3-oxo-2-phenylpyrazol-4-yl)-methylamino]methanesulfonate
	15	Lidocaine·HCl		73-78-9	2-(diethylamino)-N-(2,6-dimethylphenyl)acetamide; hydrochloride
	16	Hydroxyzine·2HCl		2192-20-3	2-[2-[4-[(4-chlorophenyl)phenyl]methyl]piperazin-1-yl]ethoxy]ethanol; dihydrochloride
	17	Levamisole·HCl		16595-80-5	(6S)-6-phenyl-2,3,5,6-tetrahydroimidazo[2,1-b][1,3]thiazole; hydrochloride
	18	Papaverine·HCl (technically not an adulterant—it is a byproduct of the heroin manufacturing process)		61-25-6	1-[(3,4-dimethoxyphenyl)methyl]-6,7-dimethoxyisoquinoline; hydrochloride
	19	Procaine·HCl		51-05-8	2-(diethylamino)ethyl 4-aminobenzoate; hydrochloride
	20	Phenacetin		62-44-2	N-(4-ethoxyphenyl)acetamide

Table S1. Trade names, structures, and IUPAC names of the compounds discussed in the paper.

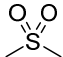
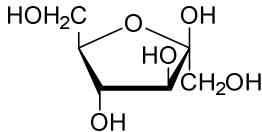
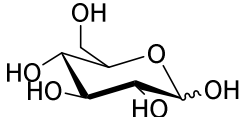
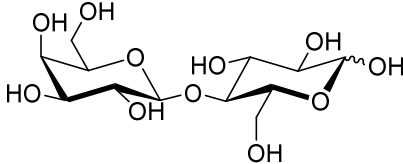
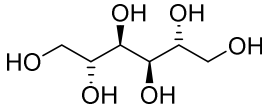
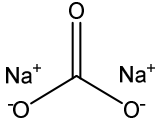
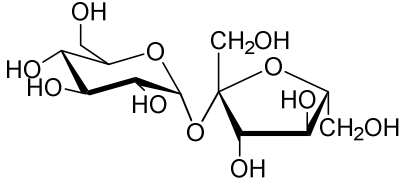
Group	Compound			CAS no.	IUPAC name
	#	Trade name	Structure		
Diluents	21	Dimethyl sulfone		67-71-0	(methanesulfonyl)methane
	22	D-Fructose		57-48-7	D-Fructose
	23	D-Glucose		50-99-7	D-Glucose
	24	α -Lactose		63-42-3	β -D-galactopyranosyl-(1 \rightarrow 4)-D-glucose
	25	D-Mannitol		69-65-8	(2R,3R,4R,5R)-hexane-1,2,3,4,5,6-hexol
	26	Sodium carbonate		497-19-8	Sodium carbonate
	27	Starch from potato	A mixture of the polysaccharides amylose and amylopectin. ^[15]	9005-25-8	Mixture of compounds
	28	Sucrose		57-50-1	β -D-Fructofuranosyl α -D-glucopyranoside
	29	Talc	$Mg_3Si_4O_{10}(OH)_2$	14807-96-6	Dioxosilane; oxomagnesium; hydrate

Table S2. The most common range of purity of illicit drugs at the retail level, and the most frequent adulterant and diluents associated with each type of drug. Note that oxycodone is a prescription drug, all other compounds are to drugs from illicit sources.

Active compound	Common range of drug content (wt%)	Most common adulterants and diluents
<i>Fentanyl</i>	US: N/A. The average is reported to be 5.1 wt% ^[16] Europe: N/A	Fentanyl is commonly found in mixtures sold as opioids, heroin, or cocaine. ^[16] Fentanyl is often mixed with sugars. ^[17]
<i>Heroin</i>	US: 6-60% ^[18] Europe: 15-41% ^[19]	US: quinine, caffeine, diltiazem, lactose, and mannitol. ^[18] Europe: caffeine and acetaminophen, and lactose. ^[18]
<i>Oxycodone</i>	US: The content of oxycodone·HCl in OxyContin varies (8-30%) for different suppliers and dosing. ^[20]	US: butylated hydroxytoluene, hypromellose, polyethylene glycol, polyethylene oxide, magnesium stearate, titanium dioxide, and compounds that gives the tablets color. ^[21]
<i>Cocaine</i>	US: 39-65% ^[16, 18] Europe: 18-33% ^[22]	US: levamisole, phenacetin, lidocaine, starch, and sodium carbonate. ^[16, 18] Europe: phenacetin, levamisole, caffeine, diltiazem, hydroxyzine and lidocaine. ^[18]
<i>Methamphetamine</i>	US: 90-96% ^[23] Europe: 36-70% ^[24]	US and Europe: dimethyl sulfone, caffeine, sugars, and acetaminophen. ^[25]

Table S3. Recommended techniques for identification of illicit drugs. The methods are ranked in categories according to the ability to identify the specific molecular structures. The categorization is defined by the international forensic organization SWGDRUG (‘Scientific Working Group for the Analysis of Seized Drugs’).^[26]

<p style="text-align: center;">Category A (Highest selectivity for molecular structure)</p>	Infrared Spectroscopy
	Mass Spectrometry
	Nuclear Magnetic Resonance Spectroscopy
	Raman Spectroscopy
	X-ray Diffractometry
<p style="text-align: center;">Category B (Intermediate Selectivity)</p>	Capillary Electrophoresis
	Gas Chromatography
	Ion-Mobility Spectrometry
	Liquid-Chromatography
	Microcrystalline Tests*
	Supercritical Fluid Chromatography
	Thin-Layer Chromatography
	Ultraviolet/Visible Spectroscopy (full spectrum)
	Macroscopic Examination (Cannabis only)
	Microscopic Examination (Cannabis only)
<p style="text-align: center;">Category C (Lowest Selectivity)</p>	Color Tests
	Fluorescence Spectroscopy
	Immunoassay
	Melting Point
	Pharmaceutical Identifiers (i.e., information on packaging)

*Chemical tests based on the addition of chemical reagents that form specific types of microcrystals when a specific drug is present. The crystals are identified by observation by light microscopy.

Table S4. The densities of different active compounds, adulterants, and diluents found in mixtures of illicit powdered drugs. The densities represent the values reported in literature, and measured with the MagLev device in this study. N/A= Not available.

	Compound	Density reported in literature (g cm ⁻³)	Density measured with MagLev* (g cm ⁻³)	%-difference in density measured with Maglev relative to reported values**
Active compounds:	Fentanyl·HCl	N/A	1.19	N/A
	Fentanyl citrate	1.23 ^[27]	N/A	N/A
	Fentanyl base	1.16 ^[28]	N/A	N/A
	Acetyl fentanyl·HCl	N/A	1.18	N/A
	Benzyl fentanyl·HCl	N/A	1.14	N/A
	Cocaine·HCl	1.34 ^[29]	1.32	5.6
	Heroin·HCl	1.38 ^[30]	1.34	-2.9
	Methamphetamine·HCl	0.91 ^[31]	1.10	20.1
Adulterants:	Acetaminophen	1.29 ^[32]	1.27	-1.6
	Caffeine	1.39 ^[33]	1.36	-2.2
	Diltiazem·HCl	1.24 ^[31]	1.30	4.8
	Dipyron / Metamizole sodium	1.39 ^[34]	1.38	-0.7
	Lidocaine·HCl	1.20 ^[32]	1.19	-0.8
	Hydroxyzine·2HCl	1.24 ^[31]	1.22	-1.6
	Levamisole·HCl	1.31 ^[31]	1.45	10.7
	Papaverine·HCl*	1.33 ^[35]	1.30	-2.2
	Procaine·HCl	1.16 ^[36]	1.23	6.0
	Phenacetin	1.24 ^[32]	1.21	-2.41
Diluents:	Dimethyl sulfone	1.44 ^[37]	1.43	-0.7
	β-D-(-)-Fructose	1.6 ^[38]	1.58	-2.5
	D-(+)-Glucose	1.54 ^[39]	1.51	-1.9
	α-Lactose	1.54 ^[40]	1.50	-2.6
	D-Mannitol	1.51 ^[41]	1.51	0
	Sodium carbonate	2.54 ^[42]	>1.77	N/A
	Starch from potato	1.5 ^[43]	1.48	-2.6
	Sucrose	1.59 ^[41]	1.58	-0.6
	Talc	2.82 ^[44]	>1.55	N/A

*The densities of the compounds are determined by recording the height (distance above the bottom magnet) that each levitating fraction levitated between the two magnets. The middle of the centroid formed by each levitating cloud is defined as the height of levitation of that particular fraction. The recorded height is converted to a value of density using an experimentally determined standard curve.

** The discrepancies in densities between the values reported in literature and measured with MagLev can be caused by different factors. For example, X-ray diffractometry is often performed on single crystals that are perfectly crystalline, illicit drug samples are known to contain compounds that are not perfectly crystalline. In addition, the densities measured with MagLev in this study were determined from levitating clouds that typically consisted of several hundred particles that in some cases were crystalline or amorphous (or a mixture of both states), or in different states of hydration or crystal polymorphism etc.

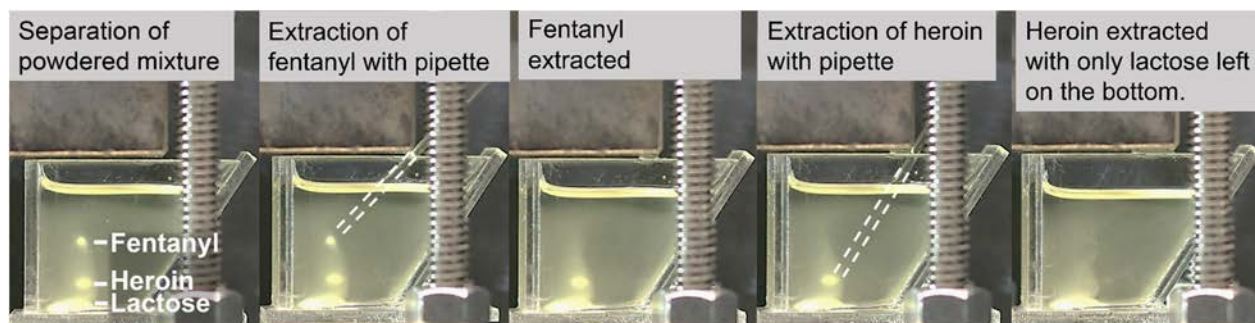
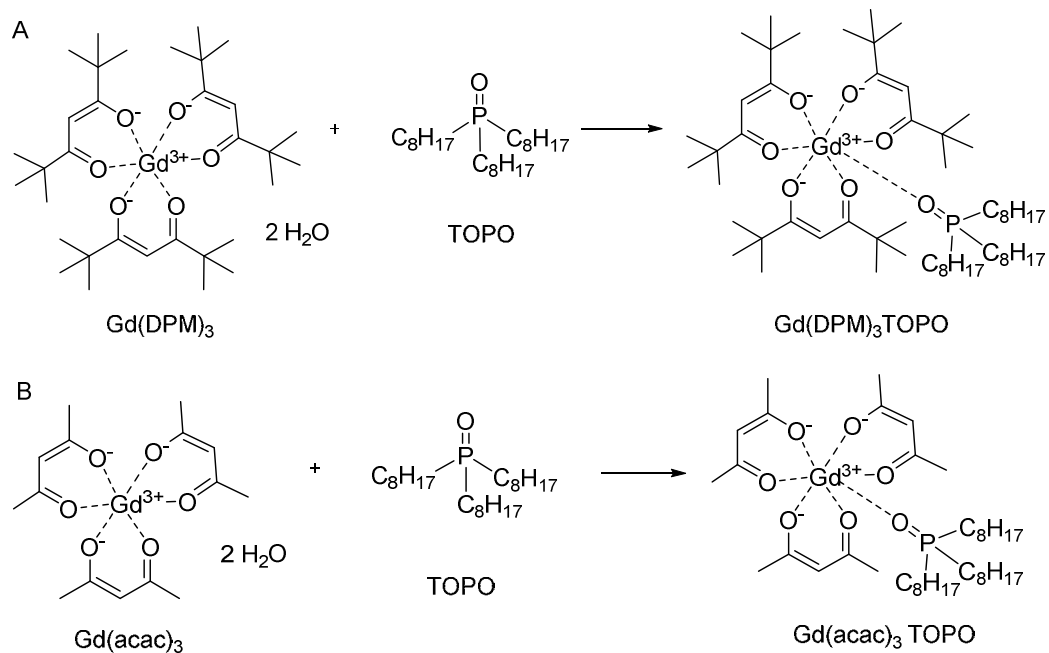


Figure S4. Separation and extraction of the separate fractions of a powdered mixture (50 mg) of fentanyl-laced heroin in a MagLev device. The powdered mixture consisted of fentanyl·HCl (1.3 wt%), heroin·HCl (2.6 wt%), and α -lactose (96 wt%—bottom of the cuvette). The mixture was allowed to separate for 30 minutes before the different fractions were extracted with a Pasteur pipette (dashed white lines). The lactose did not levitate and sank to the bottom of the cuvette. The geometric shape of the cuvette (height: 25 mm) facilitated the insertion of the pipette without disturbing the levitated solids. The paramagnetic solution consisted of $\text{Gd}(\text{DPM})_3\text{TOPO}$ (450 mM) dissolved in a mixture of 23 vol% hexane and 77 vol% tetrachloroethylene. The images were uniformly post-processed for contrast and clarity.



Scheme S1. The pathways of synthesis for the two hydrophobic complexes of gadolinium using commercially available precursors. The products are (A) tris(dipivaloylmetanato) (trioctylphosphineoxide) gadolinium(III), ($\text{Gd(DPM)}_3\text{TOPO}$; Compound **1**), and (B) tris(acetylacetonate)(trioctylphosphineoxide) gadolinium(III), ($\text{Gd(acac)}_3\text{TOPO}$; Compound **2**).

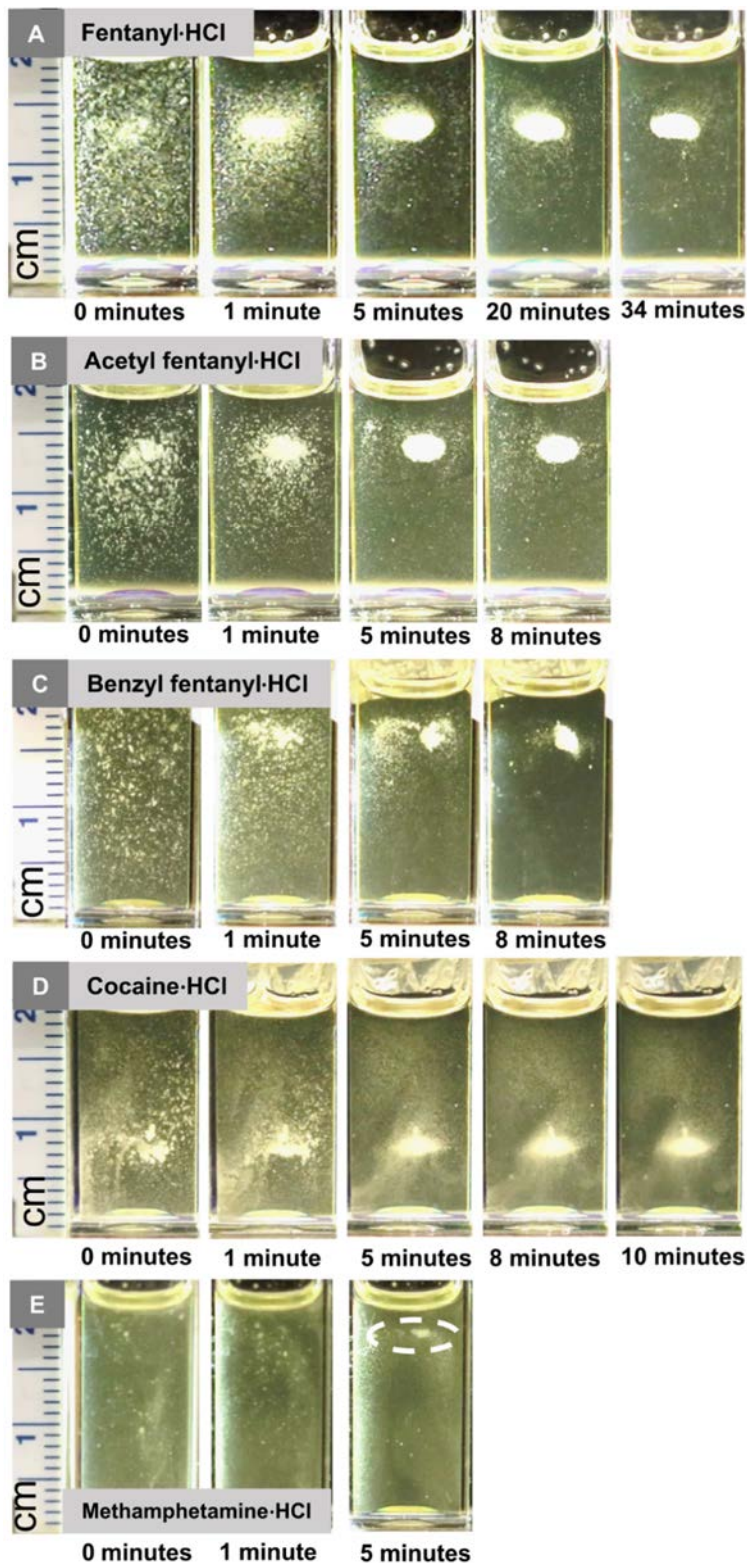


Figure S5. Time-lapse photography of individual drugs (2–9 mg of powder) levitating in a MagLev device. The paramagnetic solution consisted of $\text{Gd}(\text{DPM})_3\text{TOPO}$ (450 mM) dissolved in a mixture of 23 vol% hexane and 77 vol% tetrachloroethylene. The white dashed circle in (E) highlights the area where methamphetamine·HCl equilibrated in the MagLev. The images were uniformly post-processed for contrast and clarity.

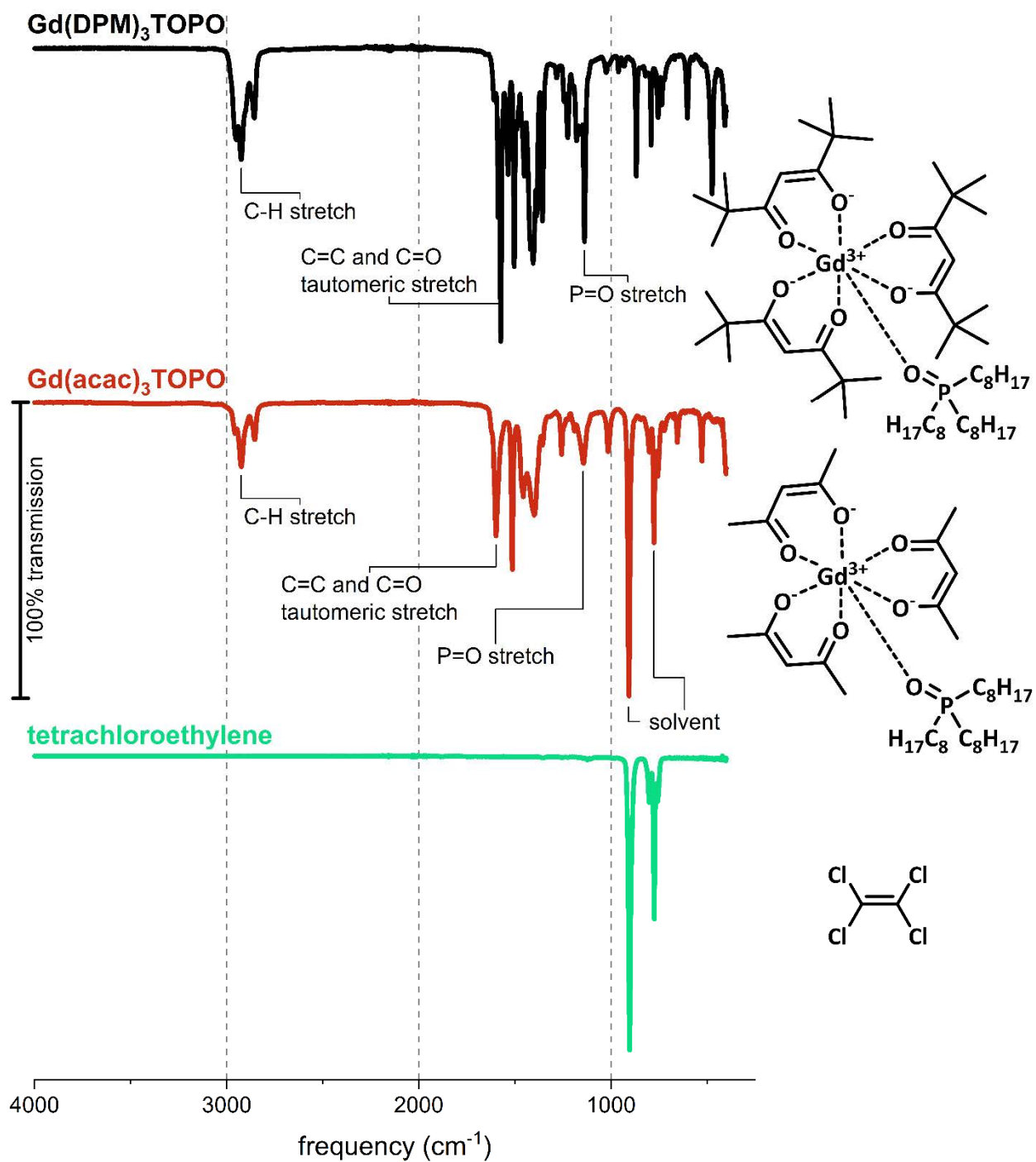


Figure S6. FTIR-ATR spectra of $\text{Gd}(\text{DPM})_3\text{TOPO}$ and $\text{Gd}(\text{acac})_3\text{TOPO}$, and the solvent tetrachloroethylene that is present as a solvent for the $\text{Gd}(\text{acac})_3\text{TOPO}$ chelate.

Assignment of peaks in the FTIR-ATR spectra of the Gd-chelate complexes:

IR-ATR (Gd(DPM)₃TOPO): 2924 cm⁻¹ (C-H stretch, m), 1573 cm⁻¹ (C=C and C=O tautomeric stretch, vs) 1137 cm⁻¹ (P=O stretch, s).

IR-ATR (Gd(acac)₃TOPO in tetrachloroethylene): 2923 cm⁻¹ (C-H stretch, m), 1598 cm⁻¹ (C=C and C=O tautomeric stretch, s), 1142 cm⁻¹ (P=O stretch, m), 906 cm⁻¹ and 776 cm⁻¹ (tetrachloroethylene solvent, s).

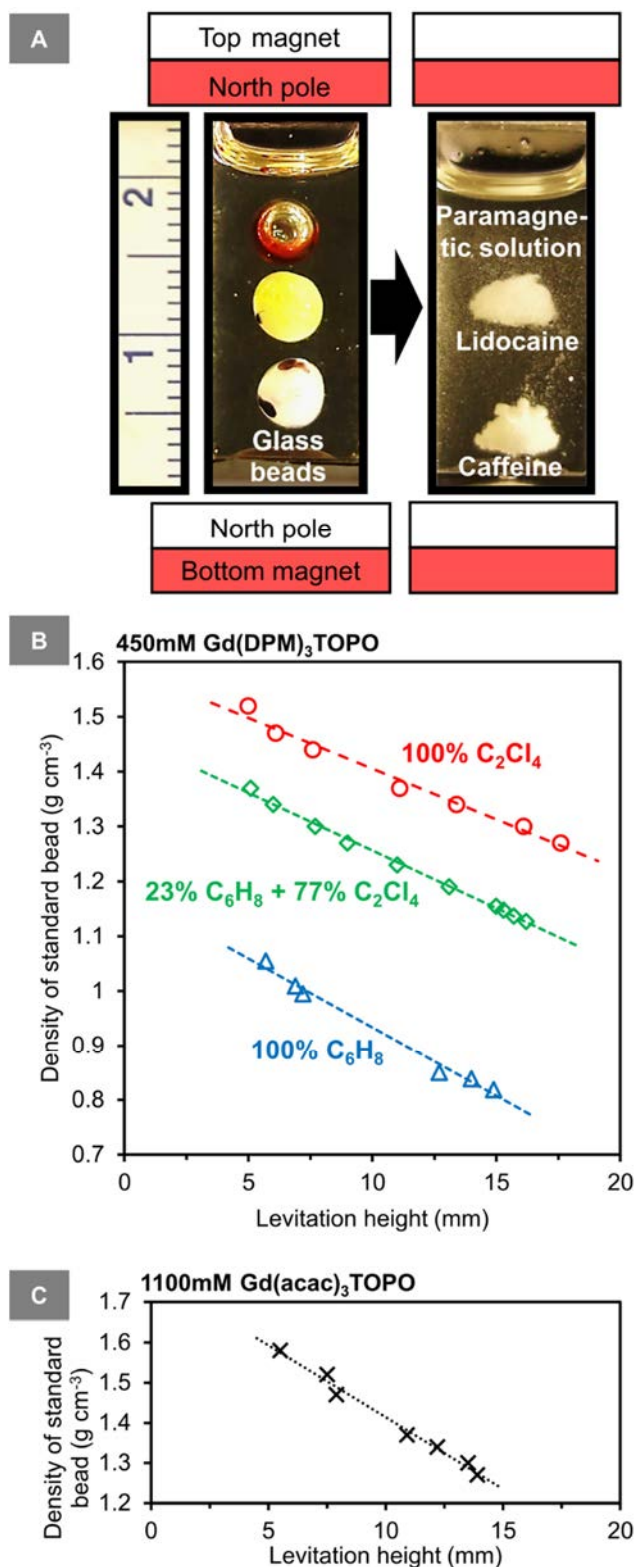


Figure S7. (A) The MagLev device is calibrated by measuring the position of glass beads of known density (with a ruler for reference). The standard curve is used to find the density of levitating fractions (i.e., here, obtained from lidocaine·HCl and caffeine) in the MagLev device. (B) Standard curves measured with glass bead density standards in solutions of Gd(DPM)₃TOPO (450 mM) dissolved in solvent mixtures of different composition (% (vol%); C₂H₈ (hexane); C₂Cl₄ (tetrachloroethylene)). (C) The standard curve measured with glass bead density standards in a solution of Gd(acac)₃TOPO (1100 mM; as obtained from the synthesis in tetrachloroethylene, without further dilution).

Table S5. Requirements for handling of schedule I and II drugs (US).^[45]

	Schedule I*	Schedule II**
Registration	Required	Required
Receiving Records	Order Forms	Order Forms
Prescriptions	No	Written prescription
Refills	No	No
Distribution Between Registrants	DEA order forms	DEA order forms
Security	Locked cabinet or other secure storage	Locked cabinet or other secure storage
Theft or Significant Loss	Report and complete DEA form	Report and complete DEA form

*Definition of Schedule I compounds (US): Drugs, compounds, and chemicals without any currently accepted use in medicine, and with a high potential for abuse, e.g., cannabis, lysergic acid diethylamide (LSD), methaqualone, peyote, heroin, and 3,4-methylenedioxymethamphetamine (ecstasy).^[45]

**Definition of Schedule II compounds (US): Drugs, compounds, and chemicals with a high potential for abuse, and a high risk of users developing strong psychological/physical dependence, e.g., fentanyl, cocaine, methamphetamine, hydromorphone, methadone, oxycodone, methadone, Ritalin, and Adderall.^[45]

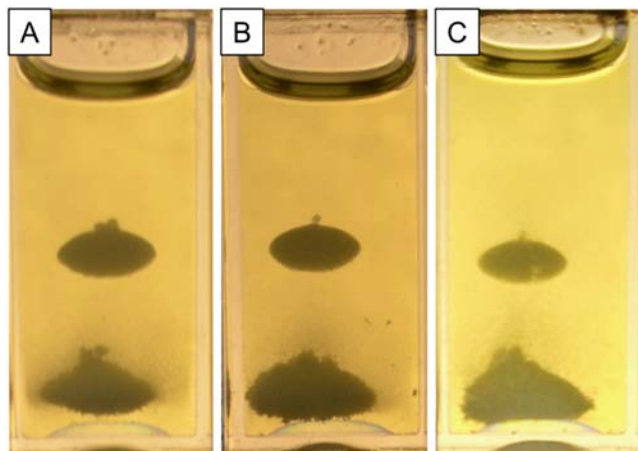


Figure S8. Separation of powdered mixtures (50:50 wt%; 45-50 mg) of lidocaine·HCl (top cloud) and caffeine (lower cloud) with MagLev using paramagnetic solutions with Gd(DPM)₃TOPO (450 mM) dissolved in the following solvent mixtures of tetrachloroethylene in combination with different n-alkanes. (A) 23 vol% heptane 77 vol% tetrachloroethylene. (B) 23 vol% octane 77 vol% tetrachloroethylene. (C) 26 vol% decane and 74 vol% tetrachloroethylene.

Original images

Figure 1A

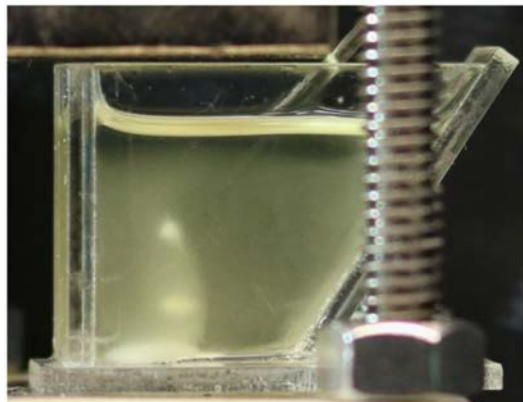


Figure 2A

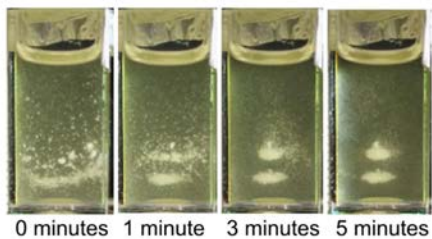


Figure 2B

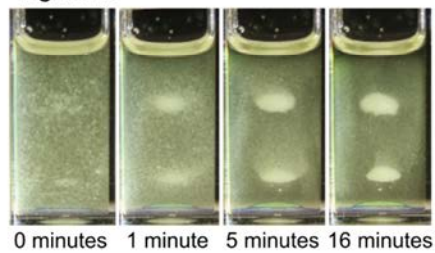


Figure 2C

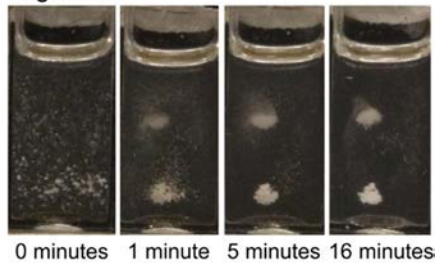


Figure 2D

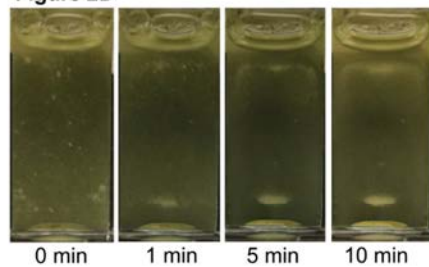


Figure 2E

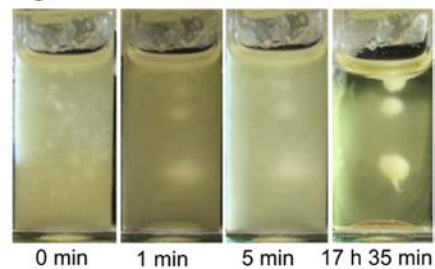


Figure 3A



Figure 3B



Figure S9. Original images (without image processing) presented in Figure 1, 2 and 4.

5. REFERENCES

- [1] a) A. Nemiroski, A. A. Kumar, S. Soh, D. V. Harburg, H.-D. Yu, G. M. Whitesides, *Anal. Chem.* **2016**, 88, 2666-2674; b) A. Nemiroski, S. Soh, S. W. Kwok, H.-D. Yu, G. M. Whitesides, *J. Am. Chem. Soc.* **2016**, 138, 1252-1257.
- [2] a) Q.-H. Gao, W.-M. Zhang, H.-X. Zou, W.-B. Li, H. Yan, Z.-K. Peng, G. Meng, *Mater. Horizons* **2019**; b) S. Ge, A. Nemiroski, K. A. Mirica, C. R. Mace, J. W. Hennek, A. A. Kumar, G. M. Whitesides, *Angew. Chem. Int. Ed.* **2019**; c) E. Turker, A. Arslan-Yildiz, *ACS Biomater. Sci. Eng.* **2018**, 4, 787-799; d) S. Yaman, M. Anil-Inevi, E. Ozcivici, H. C. Tekin, *Front. bioeng. biotechnol.* **2018**, 6; e) W. Zhao, R. Cheng, J. R. Miller, L. Mao, *Adv. Funct. Mater.* **2016**, 26, 3916-3932.
- [3] S. Ge, S. N. Semenov, A. A. Nagarkar, J. Milette, D. C. Christodouleas, L. Yuan, G. M. Whitesides, *J. Am. Chem. Soc.* **2017**, 139, 18688-18697.
- [4] K. A. Mirica, S. T. Phillips, C. R. Mace, G. M. Whitesides, *J. Agric. Food. Chem.* **2010**, 58, 6565-6569.
- [5] a) Sigma Aldrich, <https://www.sigmaaldrich.com/catalog/product/sial/371696>, May 8, **2019**; b) Sigma Aldrich, <https://www.sigmaaldrich.com/chemistry/solvents/hexane-center.html>, May 8, **2019**.
- [6] Chemsafetypro.com, https://www.chemsafetypro.com/Topics/USA/Hazardous_Materials_Identification_System_HMIS.html, May 8, **2019**.
- [7] a) K. Z. Guyton, K. A. Hogan, C. S. Scott, G. S. Cooper, A. S. Bale, L. Kopylev, S. Barone Jr, S. L. Makris, B. Glenn, R. P. Subramaniam, *Environ. Health Perspect.* **2014**, 122, 325-334; b) A. Herskowitz, N. Ishii, H. Schaumburg, *New Engl. J. Med.* **1971**, 285, 82-85.
- [8] United States Department of Labor, Occupational Safety and Health Administration, <https://www.osha.gov/dsg/guidance/perc.pdf>, **2005**.
- [9] Mathesongas.com, <https://www.mathesongas.com/pdfs/msds/MAT04310.pdf>, May 8, **2019**.
- [10] Sigma Aldrich, <https://www.sigmaaldrich.com/catalog/product/sigald/34873>, May 8, **2019**.
- [11] Sigma Aldrich, <https://www.sigmaaldrich.com/catalog/product/sial/296988>, May 8, **2019**.
- [12] <https://www.sigmaaldrich.com/catalog/product/sigald/n29406>, May 8, **2019**.
- [13] Sigma Aldrich, <https://www.sigmaaldrich.com/catalog/product/sigald/d901>, May 8, **2019**.
- [14] P. Cheng, H. Schachman, *J. Polym. Sci.* **1955**, 16, 19-30.
- [15] L. Lin, C. Cai, R. G. Gilbert, E. Li, J. Wang, C. Wei, *Food Hydrocoll.* **2016**, 52, 359-368.
- [16] U.S. Department of Justice, Drug Enforcement Administration, <https://www.dea.gov/sites/default/files/2018-11/DIR-032-18%202018%20NDTA%20final%20low%20resolution.pdf>, **2018**.
- [17] Personal Communication: J. S. Bozenko Jr, U.S. Department of Justice, Drug Enforcement Administration, January 18, **2019**.
- [18] J. Broséus, N. Gentile, P. Esseiva, *Forensic Sci. Int.* **2016**, 262, 73-83.
- [19] U.S. Department of Justice, Drug Enforcement Administration, <https://www.dea.gov/sites/default/files/2018-07/HeroinDomesticMonitorProgram.pdf>, **2015**.
- [20] R. Natarajan, *Massachusetts Lawyers Journal*, **2001**, September, 19-21.
- [21] RxList.com, <https://www.rxlist.com/oxycontin-drug.htm#description>, May 3, **2019**.

- [22] European Monitoring Centre for Drugs and Drug Addiction, http://www.emcdda.europa.eu/data/stats2017/ppp_en, **2017**.
- [23] U.S. Department of Justice, Drug Enforcement Administration, https://www.dea.gov/sites/default/files/2018-07/DIR-040-17_2017-NDTA.pdf, **2017**.
- [24] European Monitoring Centre for Drugs and Drug Addiction, 10.2810/32306, <https://publications.europa.eu/en/publication-detail/-/publication/ee6d3292-0624-44ce-a692-b12ce6cdbc12/>, **2014**.
- [25] a) U.S. Department of Justice, Drug Enforcement Administration, <https://www.justice.gov/archive/ndic/pubs1/1837/1837t.htm>, **2002**; b) <http://www.cph.org.uk/wp-content/uploads/2012/08/cut-a-guide-to-the-adulterants-bulking-agents-and-other-contaminants-found-in-illicit-drugs.pdf>, **2010**; c) European Monitoring Centre for Drugs Drug Addiction, http://www.emcdda.europa.eu/publications/joint-publications/methamphetamine_en, **2009**.
- [26] Scientific Working Group for the Analysis of Seized Drugs, http://www.swgdrug.org/Documents/Part%20IIIB_082018_CLEAN.pdf, **2018**.
- [27] O. Peeters, N. Blaton, C. De Ranter, A. Van Herk, K. Goubitz, *J. Cryst. Mol. Struct.* **1979**, 9, 153-161.
- [28] N. Ogawa, H. Nagase, T. Endo, T. Loftensson, H. Ueda, *X-Ray Struct. Anal. Online* **2009**, 25, 83-84.
- [29] E. Gabe, W. Barnes, *Acta Crystallogr.* **1963**, 16, 796-801.
- [30] E. Balchin, D. J. Malcolm-Lawes, M. D. Rowe, J. A. Smith, M. J. Bearpark, J. W. Steed, W. Wu, A. J. Horsewill, D. Stephenson, *New J. Chem.* **2004**, 28, 1309-1314.
- [31] European Network of Forensic Science Institutes, Drugs Working Group, http://enfsi.eu/wp-content/uploads/2016/09/guidelines_quant_sampling_dwg_printing_vf4.pdf, **2014**.
- [32] X. Cao, N. Leyva, S. R. Anderson, B. C. Hancock, *Int. J. Pharm.* **2008**, 355, 231-237.
- [33] H. G. Edwards, E. Lawson, M. de Matas, L. Shields, P. York, *J. Chem. Soc., Perkin Trans. 2* **1997**, 1985-1990.
- [34] H. Krishna Murthy, L. Brehm, *Acta Cryst. B: Struct. Cryst. Cryst.* **1979**, 35, 612-615.
- [35] C. Reynolds, R. Palmer, B. Gorinsky, *J. Cryst. Mol. Struct.* **1974**, 4, 213-225.
- [36] S. Kashino, M. Ikeda, M. Haisa, *Acta Cryst. B: Struct. Cryst. Cryst.* **1982**, 38, 1868-1870.
- [37] D. E. Sands, *Z. Kristallogr. Cryst. Mater.* **1964**, 119, 245-251.
- [38] J. Kanters, G. Roelofsen, B. Alblas, I. Meinders, *Acta Cryst. B: Struct. Cryst. Cryst.* **1977**, 33, 665-672.
- [39] W. Ferrier, *Acta Crystallogr.* **1963**, 16, 1023-1031.
- [40] W. Roelfsema, B. Kuster, M. Heslinga, H. Pluim, M. Verhage, Wiley, New York, **2010**.
- [41] J. Elversson, A. Millqvist-Fureby, *J. Pharm. Sci.* **2005**, 94, 2049-2060.
- [42] M. Dušek, G. Chapuis, M. Meyer, V. Petricek, *Acta Crystallogr. B Struct. Sci.* **2003**, 59, 337-352.
- [43] A. Buléon, P. Colonna, V. Planchot, S. Ball, *Int. J. Biol. Macromol.* **1998**, 23, 85-112.
- [44] J. W. Gruner, *Z. Kristallogr. Cryst. Mater.* **1934**, 88, 412-419.
- [45] U.S. Department of Justice, Drug Enforcement Administration, https://www.deadiversion.usdoj.gov/pubs/manuals/pract/pract_manual012508.pdf, **2006**.

6. AUTHOR CONTRIBUTIONS

C.K.A. conceived the research, performed the MagLev separations, and data analysis. A.N. conceived compound 2, and synthesized and characterized compound 1 and 2. M.J.F. synthesized compound 1, analyzed data, and prepared figures and movies. D.J.P. performed the imaging with SEM. S.G. made the MagLev device, performed simulations and created Figure S2. J.S.B. performed MagLev separations and FTIR-ATR measurements. C.K.A., M.J.F., and G.M.W wrote the manuscript. G.M.W. supervised the research. All authors contributed to editing the final manuscript.